Molecular dynamics simulations of a polymer chain

Eyob Tewelde

December 17, 2024

1. Introduction

Space exploration has received increasing attention over the last few decades to support the long-term development of humanity[1]. The use of polymers in space technology, such as thermal control coatings, seals, adhesives, etc., has received similar attention due to their toughness, elasticity, electrical resistance, and a large range of other desirable properties[2,3]. However, the extreme conditions of space, such as near 0 K temperatures, can degrade polymers, thereby reducing the lifespan and reliability of spacecraft technology[4]. Therefore, it is important to study the behavior of polymers at low temperatures to understand their phase transitions into folded states as well their dependence on the repulsive interactions between molecules of the polymer to improve the capabilities of spacecraft. In this report, molecular dynamics (MD) simulations were run to understand the folding behavior of a polymer as a function of temperature and repulsive energies. The end-to-end distance, gyration ratio, and potential energy of the final configurations for each simulation were compared to determine the conditions to prevent polymer folding. An understanding of this behavior will allow for advancements in the design and testing of new polymers that can withstand the conditions of space travel.

2. Methods

Molecular dynamics (MD) simulations were used to study the evolution of a polymer as a function of temperature. The systems were modeled using a harmonic force potential to calculate the interactions between neighboring particles (**Eq. 1**) and an attractive (**Eq. 2**) and repulsive (**Eq. 3**) Lennard-Jones (LJ) potential to model the interactions between particles that were one and two spacers apart, respectively (**Fig. 1**).

$$U_{bond}(r) = \frac{1}{2}k(r - r_0)^2 \tag{1}$$

$$\mathrm{U_{LJ,att}}(r) = 4\varepsilon_{\mathrm{att}}\left[\left(\frac{\sigma}{\mathrm{r}}\right)^{12} - \left(\frac{\sigma}{\mathrm{r}}\right)^{6}\right] \tag{2}$$

$$U_{LJ,rep}(r) = \begin{cases} 4\varepsilon_{\mathrm{rep}}\left[\left(\frac{\sigma}{\mathrm{r}}\right)^{12} - \left(\frac{\sigma}{\mathrm{r}}\right)^{6} + \frac{1}{4}\right], & r < 2^{1/6}\sigma \\ 0, & x \geq 2^{1/6}\sigma \end{cases} \tag{3}$$

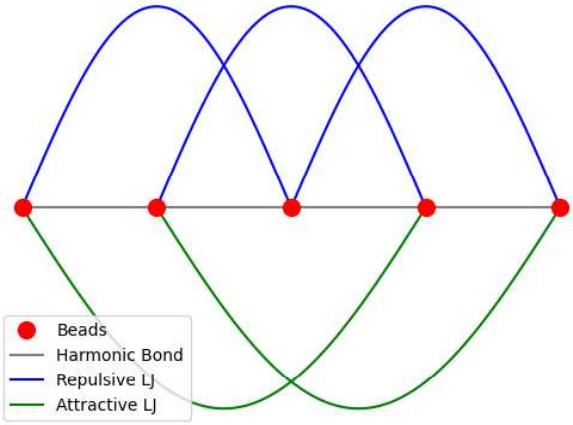

Fig 1. Simple representation of the distance-dependent potential for the polymer

Three parameter sets were created to calculate the gyration ratio, end-to-end distance, and total potential energy as a function of temperature *T*, the depth of the repulsive LJ potential, and the spring constant *k*. Within each parameter set, ten simulations were run. In each system, 20

particles were initialized with random Cartesian coordinates such that neighboring particles in the chain were separated by 1 Å. Periodic boundary conditions were applied so that a particle's coordinates remained within the simulation box. The velocities of the particles were sampled from a Maxwell-Boltzmann distribution corresponding to the system temperature. Each system was allowed to evolve for 10,000 steps with one step equaling 0.01 reduced time units. During each step, the harmonic (**Eq. 1**) and Lennard-Jones potentials (**Eqs. 2-3**) for each particle was calculated. The forces arising from the potentials were calculated and applied to each particle (**Eqs. 4-6**), from which the velocities and positions of each particle were updated.

$$F_{harm}(r) = -k(r - r_0)\hat{r} \tag{4}$$

$$F_{LJ,rep}(r) = 24\varepsilon_{\text{rep}}\left[\left(\frac{\sigma}{\text{r}}\right)^{12} - 0.5\left(\frac{\sigma}{\text{r}}\right)^{6}\right] * \frac{\hat{r}}{r} \tag{5}$$

$$F_{LJ,att}(r) = 24\varepsilon_{\text{att}}\left[\left(\frac{\sigma}{\text{r}}\right)^{12} - 0.5\left(\frac{\sigma}{\text{r}}\right)^{6}\right] * \frac{\hat{r}}{r} \tag{6}$$

After the velocities were updated, a rescaling factor (**Eq. 7**) was applied to the velocity of each particle to ensure that the velocities followed a Maxwell-Boltzmann distribution of the initial temperature, where T_{inst} is shown in **Eq. 8**. After the simulation for each system was complete, the radius of gyration (**Eq. 9**), the end-to-end distance (**Eq. 10**), and the sum of the harmonic, attractive LJ, and repulsive potential energies were calculated. The trajectories were visualized using OVITO.

3. Results

3.1 Polymer folding as a function of temperature

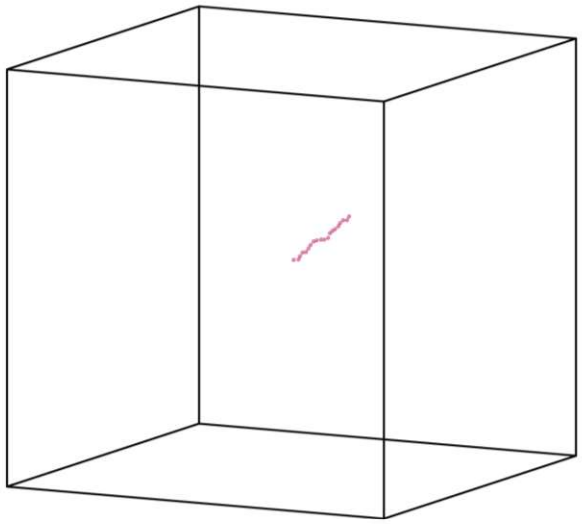

Fig 2. Initial polymer configuration

The simulation relating polymer folding as a function of temperature was run with parameters k = ε_{rep} = 1. The initial configuration for the polymers for all systems is shown in **Fig. 2**. The final configuration of the polymer at the minimum temperature, T = 0.01 and the maximum temperature, T = 1 is shown in **Figs. 3a-b**. The trajectories of the simulations conducted at all temperatures do not indicate a clear phase transition. The end-to-end distance tends to increase as a function of temperature, but the relationship is unclear. (**Figs. 4a**).

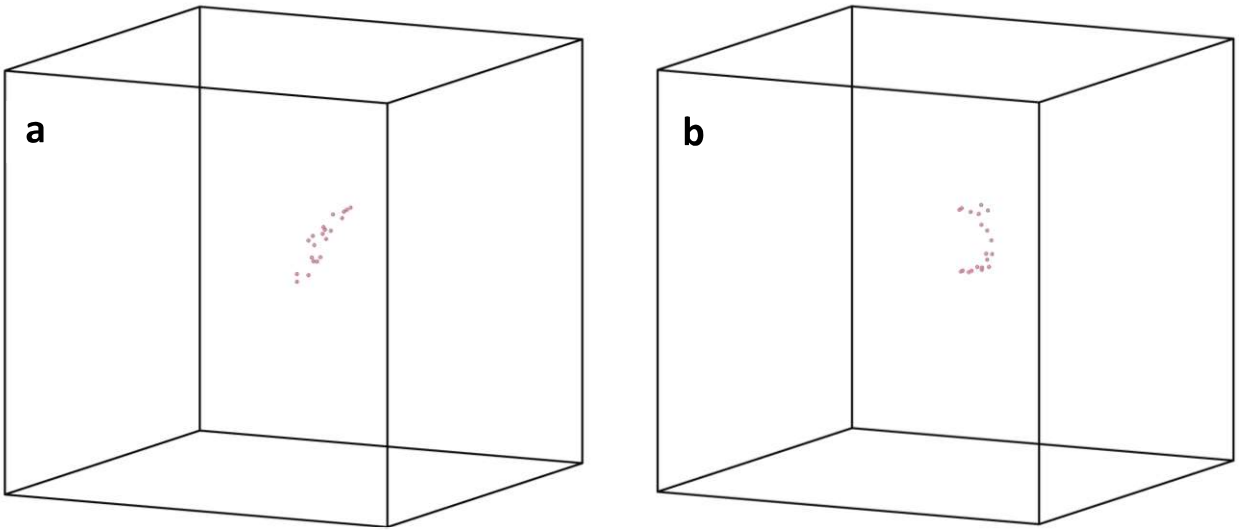

Fig 3. a) Final configuration at T = 0.1 and **b)** T = 1

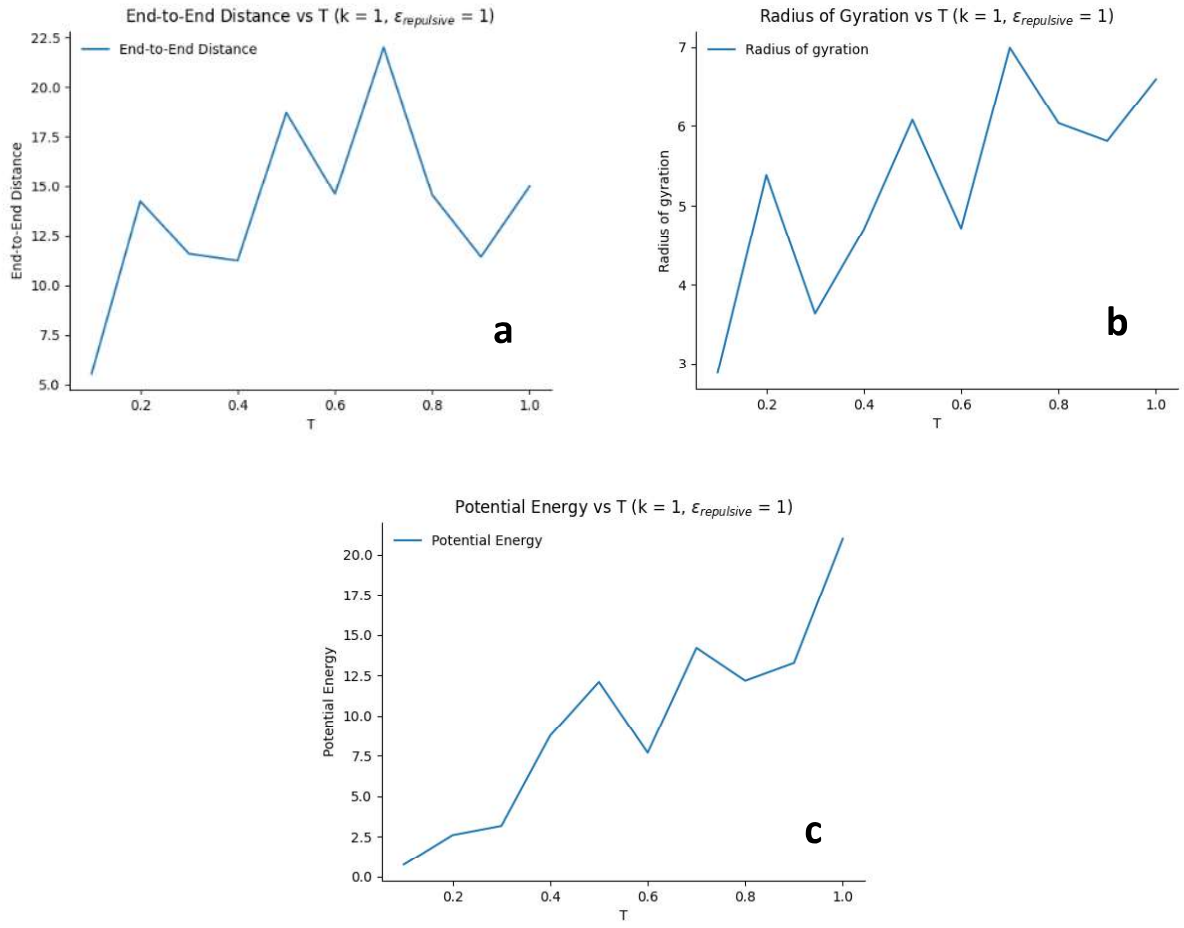

Fig 4. **a)** End-to-end distance, **b)** radius of gyration, and **c)** potential energy of the final configuration of the polymers as a function of T.

On the other hand, the potential energy and the gyration ratio clearly increased as a function of temperature (**Figs. 4b-c**). However, neither provide evidence for a temperature-based phase transition since both properties alternate between increasing and decreasing values.

3.2 Polymer folding as a function of ε_{rep}

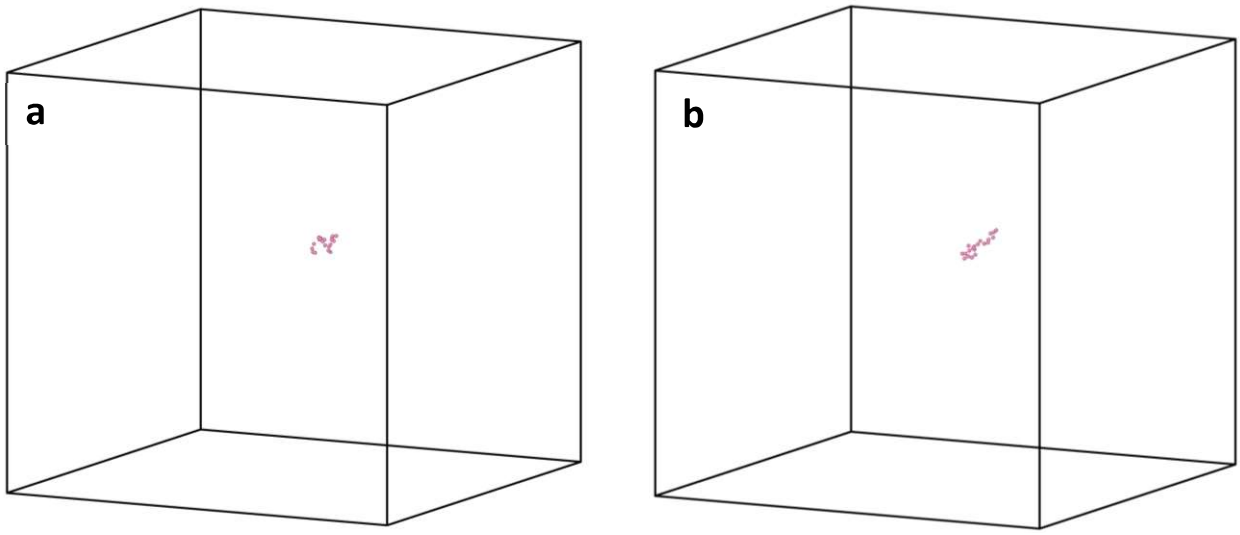

Fig 5. a) Final configuration of polymers at ε_{rep} = 0 and **b)** ε_{rep} = 2.

The simulation that studied the relationship between polymer folding and ε_{rep} was conducted at k = 1 and T = 0.1. The final configurations of the polymers at the minimum ε_{rep} = 0 and maximum ε_{rep} = 2 are shown in **Figs. 5a-b**. The trajectories of intermediate values of ε_{rep} do not show a clear phase transition from a folded to an unfolded polymer phase. Similarly, the end-to-end distance, gyration ratio, and potential energy do not suggest a phase transition in the polymer as a function of ε_{rep} (**Figs. 6a-c**).

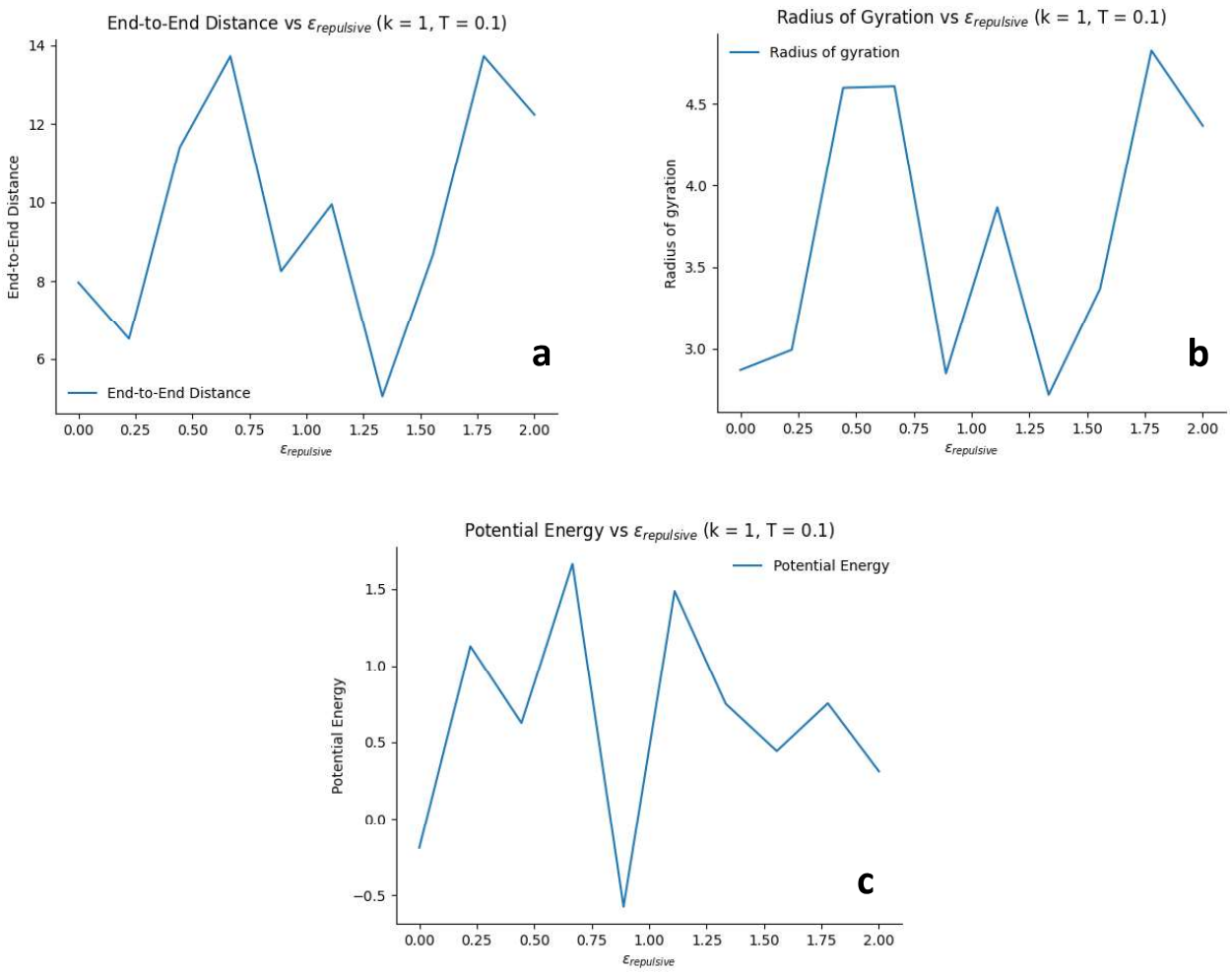

Fig 6. **a)** End-to-end distance, **b)** radius of gyration, and **c)** potential energy of the final configuration of the polymers as a function of ε_{rep}.

3.3 Polymer folding as a function of k

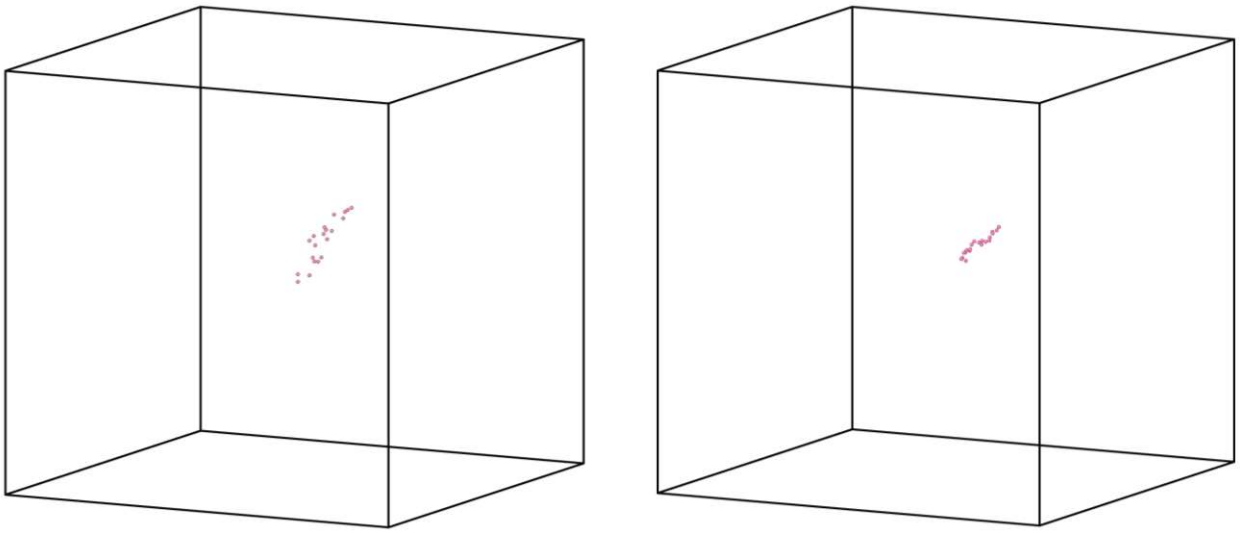

Fig 7. a) Final configuration of polymers at k = 0.1 and **b)** k = 2.

The final configurations of the polymers at the minimum k = 0.1 and k = 2 are shown in **Figs. 7a-b**. Contrary to the trajectories observed in **3.1** and **3.2**, the trajectories of the polymers clearly became more folded as k increased. This is validated by the decrease of the end-to-end distance and gyration ratio as a function of k in **Figs. 8a-b**. It is also observed that potential energy decreases as a function of k (**Fig. 8c**). This decrease in potential energy only occurs in the parameter set where k is varied.

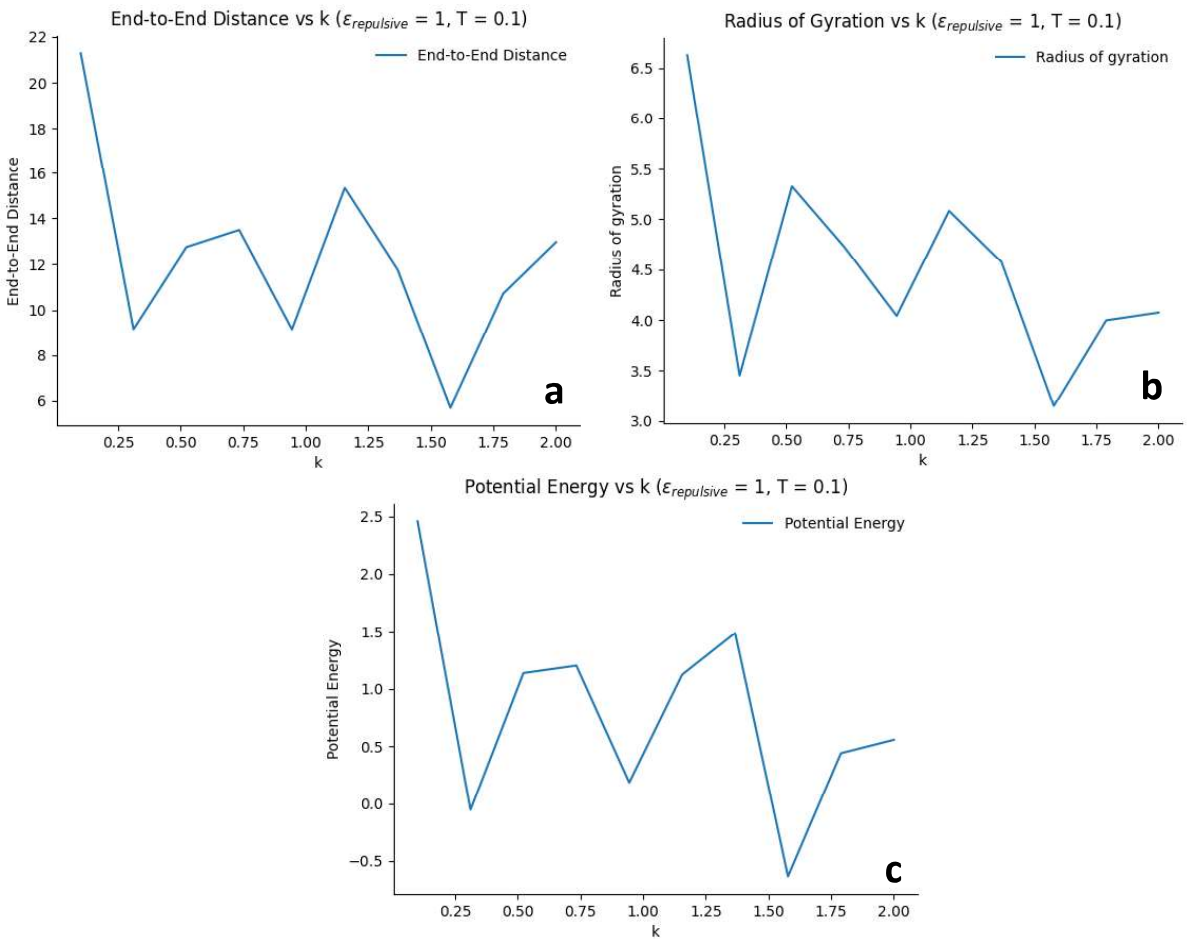

Fig 8. **a)** End-to-end distance, **b)** radius of gyration, and **c)** potential energy of the final configuration of the polymers as a function of k.

4. Discussion

4.1 Impact of temperature on polymer folding

The plots in **Figs. 4a-c** show that, while not a consistent trend, the polymer unfolding occurs at higher temperatures. An increase in the end-to-end distance can be attributed to an increase in folding since the end-to-end distance will be maximized for a fully unfolded state. However, it should be noted that there can be cases where a polymer is generally unfolded throughout its structure, but the ends are curved towards each other (**Fig. 3b**), reducing the end-to-end distance. This suggests that the end-to-end distance cannot solely be used to study polymer unfolding and it also helps to explain why the trends in end-to-end distance for all parameter sets do not change monotonically. The gyration ratio, which is a measure of the average distance of the particles from the center of mass, allows for a slightly more accurate description of the polymer folding since the case described above has less of an effect on the gyration ratio. This can explain why the changes in gyration ratio are much less intense then the changes in end-to-end distance. Regardless, both show that the polymer tends to unfold over time. Furthermore, the increase in potential energy shows that the directions of the bonds begin to align as the temperature increases. The potential energy can only increase from the harmonic potential, since both LJ potentials approach 0 at long distances. Since the harmonic potential increase as a function of r, the potential energy plot suggests that r increases as a function of temperature.

Although the simulations show that the polymer tends to unfold at increasing temperatures, there is no evidence for a phase transition from a folded to an unfolded state. If there was a phase transitions, all of the plots **in Figs. 4a-c** would show two distinct regimes in

which past some temperature, the end-to-end distance and gyration ratio would be clearly larger than at the temperatures before it. Since this is not shown, a phase transition cannot be confidently assigned.

4.2 Impact of ε_{rep} on polymer folding

The simulations that varied ε_{rep} provided the least amount of interpretable data. While **Figs. 6a-c** show that the maximum ε_{rep} results in a higher end-to-end distance, gyration ratio, and potential energy than the minimum ε_{rep}, the apparent randomness in these measurements across all values of ε_{rep} suggest that there is an error in the simulation setup that needs to be accounted for in future studies. Since **Eq. 5** was used to calculate the forces arising from the repulsive LJ potential, in which a clear direct relationship between polymer folding and ε_{rep} should be observed, there was likely a mistake in the position updates of the simulation. Additionally, it makes intuitive sense that for stronger repulsive interactions, a polymer is more likely to adopt a state the minimizes interactions with other particles, which would occur through polymer unfolding.

4.2 Impact of k on polymer folding

The spring constant, k, was shown to decrease the end-to-end distance, gyration ratio, and potential energy of the polymers, suggesting that k promotes polymer folding (**Figs. 8a-c**). However, similar to the effect of temperature on polymer folding, this claim is made sparingly

since the trend is not consistent across all values of k. This concurrent theme suggests that this report would benefit greatly by sampling larger parameter sets as well as running for more steps.

Regardless, based on the data in **3.2** and **3.3,** $\varepsilon_{rep} = 2$ and k = 0.1 should be used to prevent polymer folding.

5. Conclusion

The simulations run in this report do not provide accurate enough results to form strong conclusion on the parameters for desirable polymer design. As mentioned briefly, the erratic calculations and unintuitive results suggest an error lie in the simulation design. More work needs to be done to either update the simulation design or to make sense of the unintuitive impact of ε_{rep}. However, if we assume these errors did not carry over in the simulations that varied temperature and the spring constant, then we conclude that polymer unfolding occurs with an increase in temperature and a decrease in the spring constant. The relationship between the spring constant suggests that polymers with weaker bonds are more likely to be in an unfolded state. This observation shows that, while polymers with incredibly strong bonds might be resistant to degradation in the face of certain space conditions, such as high energy light, it comes at the cost of being brittle. Therefore, the main conclusion of this report is that it is of some use to design polymers with relatively weaker bonds.

References

1. Mathieu, E. & Roser, M. Space Exploration and Satellites. *Our World in Data* (2023).
2. Willis, P. B. & Hsieh, C.-H. Space Applications of Polymeric Materials. *Kobunshi* **49**, 52–56 (2000).
3. Chen, J., Ding, N., Li, Z. & Wang, W. Organic polymer materials in the space environment. *Progress in Aerospace Sciences* **83**, 37–56 (2016).
4. Wu, W., Liu, W., Qiao, D. & Jie, D. Investigation on the development of deep space exploration. *Sci. China Technol. Sci.* **55**, 1086–1091 (2012).